ORIGINAL RESEARCH

In silico and in vivo characterization of cabralealactone, solasodin and salvadorin in a rat model: potential anti-inflammatory agents

Arif Malik[1]
Mahwish Arooj[2]
Tariq Tahir Butt[3]
Sara Zahid[4]
Fatima Zahid[1]
Tassadaq Hussain Jafar[1]
Sulayman Waquar[1]
Siew Hua Gan[5]
Sarfraz Ahmad[1]
Muhammad Usman Mirza[6]

[1]Institute of Molecular Biology and Biotechnology (IMBB), University of Lahore, Lahore, Pakistan; [2]University College of Medicine and Dentistry (UCMD), University of Lahore, Lahore, Pakistan; [3]Khawaja Muhammad Safdar Medical College, Sialkot, Pakistan; [4]Faculty of Pharmacy, University of Lahore, Lahore, Pakistan; [5]School of Pharmacy, Monash University Malaysia, Subang Jaya, Malaysia; [6]Department of Pharmaceutical and Pharmacological Sciences, Rega Institute for Medical Research, Medicinal Chemistry, University of Leuven, Leuven, Belgium

Correspondence: Arif Malik
Institute of Molecular Biology and Biotechnology (IMBB), University of Lahore, 1 Km Defense Road Off Raiwind Road, Lahore 54000, Pakistan
Mob +92 0321 844 8196
Email arifuaf@yahoo.com

Background: The present study investigates the hepato- and DNA-protective effects of standardized extracts of *Cleome brachycarpa* (cabralealactone), *Solanum incanum* (solasodin), and *Salvadora oleioides* (salvadorin) in rats.

Materials and methods: Hepatotoxicity was induced with intraperitoneal injection of carbon tetrachloride (CCl_4) (1 mL/kg b.wt.) once a week for 12 weeks. The hepato- and DNA protective effects of the extracts in different combinations were compared with that of a standard drug Clavazin (200 mg/kg b.wt.). Tissue alanine aminotransferase, alpha-fetoprotein, tumor necrosis factor alpha (TNF-α), isoprostanes-2α, malondialdehyde, and 8-hydroxydeoxyguanosine, the significant hallmarks of oxidative stress, were studied.

Results: Histopathological findings of the liver sections from the rat group which received CCl_4+cabralealactone, solasodin, and salvadorin demonstrated improved centrilobular hepatocyte regeneration with moderate areas of congestion and infiltration comparable with Clavazin. For in silico study, the identified compounds were subjected to molecular docking with cyclooxygenase-2 and TNF-α followed by a molecular dynamics study, which indicated their potential as anti-inflammatory agents.

Conclusion: Cabralealactone, solasodin, and salvadorin confer some hepatoprotective and DNA-damage protective effects against CCl_4-induced toxicity. They successfully restored the normal architecture of hepatocytes and have the potential to be used as inhibitor to main culprits, that is, cyclooxygenase-2 and TNF-α. They can combat oxidative stress and liver injuries both as mono and combinational therapies. However, combination therapy has more ameliorating effects.

Keywords: cabralealactone, solasodin, salvadorin, antioxidant, COX-2 inhibitor, anti-inflammatory

Introduction

Currently, more than 10% of humans are affected by continuous exposure to hepatotoxic mediators like alcohol, viruses, toxic substances, and biotransformed metabolites, which may contribute to the development of liver cirrhosis and hepatocellular carcinoma.[1] Liver is an organ, which is at higher risk for toxic metabolic reactions that lead to chronic liver inflammation, mainly associated with the innate defense system of the biological organization for elimination of toxic metabolites. Elevation of liver enzymes (alanine aminotransferase [ALT], aspartate aminotransferase, gamma-glutamyl transferase, and alkaline phosphatase) is a useful indicator of an abnormal hepatic functioning in addition to the clinical manifestations seen.[2] Since hepatotoxicity is associated with inflammation and oxidative stress, herbal extracts with potent anti-inflammatory

and anti-oxidative properties are known to have therapeutic values in the treatment of fibrosis and toxic injuries. Therefore, the herbal extracts may be potential sources of new chemical metabolites with good therapeutic potential in xenobiotic-induced liver injuries.[1,2]

Cleome brachycarpa belongs to the *Cleomaceae* family and is locally known as Ponwar. It grows widely in sandy regions of Africa (especially in North Africa) and Asia (particularly in Egypt, Saudi Arabia, Afghanistan, Pakistan, India, and Iran). The plant is also known as spider flower because of its flower shape.[3] *C. brachycarpa* is reported to have some amazing biochemical activities in the biological system such as antimicrobial, hepatoprotective, anticancer, antiviral, analgesic, antiemetic, immuno-modulatory, and antioxidant properties.[4] It is also used in the Iranian traditional medicine in the treatment of jaundice, diarrhea, bronchitis, scabies, malaria, heart failure, immune system deficiency, seizure and rheumatoid arthritis, fever, chills, and stomach disorders, although in high doses, it has been reported to induce stomach swelling.[5,6] Moreover, in a recent study, the ethanolic extract of its stems, roots, and leaves shows some antioxidant effects.[7] The total phenolic and flavonoid contents of these parts are also reported to be active against 1,1-diphenyl-2-picrylhydrazyl (DPPH) radical scavenging and ferric reducing ability of plasma activities.[8] Another research established in vitro antibacterial effects of aerial parts,[9] memory-boosting effects in Alzheimer,[10] and anxiolytic effects in the central nervous system.[7] Aerial parts of plant may show cytotoxic effects because of its constituents i.e., flavonoid and sesqiterpene.[11] Spectroscopic analysis reveals that 90% of its ethanolic extract contains active phytochemical constituents, including cabralealactone (5.1%), trinortriterpenoid dilactone (0.6%), deacetoxybrachycarpone (1.1%), and ursolic acid (0.2%).[7,12] In 2010, the anticancer activity of ethanolic extract of *C. brachycarpa* was evaluated by using albino mice against Ehrlich Ascites Carcinoma cell line in 2 doses (200 and 400 mg/kg) for 9 consecutive days. The anticancer effect was evaluated by observing the tumor volume, viable tumor cell count, and hematological parameters. All the above-mentioned parameters showed a significant ($p < 0.01$) decrease and the life span of the tumor-bearing host showed an increase, indicating that the plant extract has a potential anticancer activity.[11]

Solanum incanum is locally known as thorn apple or bitter apple, an important plant utilized in Pakistan. It grows abundantly in Africa and is also found in the Middle East and India. All the parts of the plant are valued since they are mainly used to combat liver pain, ulcer, and benign tumors.[13]

Isolation of solasodin metabolite from *S. incanum* berries indicates the presence of a chemical structure related to that of a steroidal glycol-alkaloid, which can confer a protective effect against carbon tetrachloride (CCl_4)-induced hepatic insult. Cytotoxic investigation of solasodin indicates the suppressive and apoptotic characteristic against hepatitis (specifically HepG2 and Hep3B) cell lines.[14] The anti-cancer effect of the herb is mainly attributed due to its glycosidal alkaloids.[15–17] It has been reported that solasodin causes necrosis of cancer cells via upregulation of tumour necrosis factor (TNF) receptor and activation of intrinsic mitochondrial apoptotic signaling pathways.[18,19] Studies have reported the hepatoprotective effect of fresh tuber roots of *S. incanum* on CCl_4-induced liver damage.[20]

Salvadora oleoides or locally known as "Mitha Jall or Peelu" is an evergreen plant found in India and Pakistan, as well as in Southern Iran. It is traditionally used in the treatment of enlarged spleen, rheumatism, low fever, snake bites, and cough, alongside its widespread use as a purgative.[21] Two compounds, octadecanoyl heptanoate and δ-lactone of 3 isobutyl-5 hydroxy-19-oxononadeconic acid have been isolated from its stem bark, and salvadorin, a new dimeric dihydroisocoumarin has been isolated from chloroform fraction of *S. oleoides*.

Gas chromatography and mass spectrometry analysis of essential oils based on analysis of hydro-distilled extracts indicated the presence of 35 (94.0%) and 25 (91.1%) compounds in the leaf and stem, respectively. The leaf was found to contain high concentrations of 2-methoxy-4-vinylphenol (25.4%), cis-3-hexenyl benzoate (16.8%), phytol (13.9%), n-hexadecanoic acid (6.9%), and trans-β-damascenone (2.1%). On the other hand, the stem oil contains high concentrations of 2-methoxy-4-vinylphenol (21.6%), phytol (12.9%), n-hexadecanoic acid (3.6%), octacosane (7.9%), nonacosane (7.3%), 1-octadecene (5.8%), heptacosane (5.9%), hexacosane (4.5%), pentacosane (3.4%), squalene (3.9%), and trans-β damascenone (2.3%).[22]

A study was conducted to evaluate the hepatoprotective activity induced in albino rats following administration of *S. oleioides* aqueous extract. The extract significantly elevated the high-density lipoprotein (HDL) cholesterol level and decreased serum glucose, total cholesterol (TC), triglycerides, low-density lipoprotein (LDL) cholesterol, TC/HDL, and LDL/HDL ratios while the body weight, liver function indices, and selected tumor markers were approximately comparable with the control animals. These findings suggest that *S. oleioides* extract is very potent in ameliorating liver injury.[23] New technological advances have

been employed to evaluate the pharmacological properties of natural products using state-of-the-art computer-based approach, the use of which has become inevitable in drug discovery pipelines due to molecular docking and molecular dynamics simulations.[24–26] The combination of such molecular modeling techniques alongside investigation of biological activity is an important approach in elucidating novel plant-based drugs.[27] Additionally, although many natural products are widely utilized in folk medicine, their toxic potentials have not been reported. Considering these factors, the aim of the current study is to evaluate the protective effects of *C. brachycarpa* (cabralealactone), *S. incanum* (salvadorin), and *S. oleioides* (solasodin) against DNA damage and confirm their hepatoprotective effects.

Materials and methods

All chemicals and reagents used were of analytical grades and were purchased from Sigma Chemical Co. (St Louis, MO, USA). Standardized 90% ethanolic extracts of cabralealactone, 80% ethanolic extracts of both salvadorin and solasodin were purchased from Sigma Chemical Co. Ethical approval was obtained from the Institutional Review Board of The University of Lahore (Approval No: USM/Animal Ethics approval/2009/[45] [140]) and all animal experiments were performed in accordance with the Institutional Guidelines for the Care and Use of Animals for Scientific Purposes. A *p*-value of <0.05 was considered as statistically significant.

The animals were divided into several groups and received different treatments (Table 1). Subcutaneous injection of CCl₄ (1:1 v/v) was administered with saline (1 mL/kg b.wt. per week) to albino rats (*Rattus norvegicus*) every week for 12 consecutive weeks to induce hepatocellular injury as confirmed by the liver function tests.[23] At the end of the

Table 1 Experimental design

Groups (n=5)	Treatments
A	Control
B	CCl₄ alone
C	CCl₄+cabralealactone
D	CCl₄+solasodin
E	CCl₄+salvadorin
F	CCl₄+cabralealactone+solasodin
G	CCl₄+cabralealactone+salvadorin
H	CCl₄+solasodin+salvadorin
I	CCl₄+cabralealactone+solasodin+salvadorin
J	CCl₄+Clavazin

Notes: Dose of CCl₄ (1 mL/kg b.wt. per week). Dose of cabralealactone, solasodin, salvadorin (100 mg/kg b.wt.). Dose of Clavazin (200 mg/kg b.wt.).
Abbreviation: CCl₄, carbon tetrachloride.

experiment, the animals were sacrificed by an intraperitoneal injection of ketamine (Arevipharma GmbH, Radebeul, Germany) (1 mL/g).

Following sacrifice, the liver lobes were separated and collected in glass tubes containing 5% formalin for histopathology examination. For homogenate preparation, freshly dissected liver tissue was homogenized in phosphate buffer (50 mM, pH 7.2), centrifuged at 3,000 rpm for 10 min and the supernatant separated to yield 25% (w/v) homogenate. It was stored at $-80°C$ until biochemical analysis. The estimation of alanine aminotransferase (ALT) was conducted by using a commercially available Bio Merux and Randox kit.[28] The levels of α-fetoprotein (AFP), 8-hydroxy-2-deoxyguanosine (8-OHdG), tumor necrosis factor alpha (TNF-α), and isoprostanes-2 alpha (isoP-2α) were determined by using commercially available ELISA kits (Abcam, Cambridge, MA, USA).

Lipid peroxidation in the blood samples was estimated calorimetrically by measuring thiobarbituric acid reactive substances (TBARS).[29] Briefly, sample (0.2 mL), sodium dodecyl sulfate (8.1%, 0.2 mL), acetic acid (20%, 1.5 mL), and thiobarbituric acid (0.8%, 1.5 mL) were mixed, followed by centrifugation (3,000 rpm for 10 min). The upper organic layer was aspirated, and the optical density was read at 532 nm using a spectrophotometer (Echelle; LTB Lasertechnik Berlin Gmbh, Berlin, Germany) against the blank. The levels of lipid peroxides were expressed as millimoles of TBARS/g of liver tissue based on a standard curve. DPPH scavenging activity of plant extracts was measured to investigate their antioxidant status.[30] Ethanolic DPPH was added to the prepared stirred utions with the plant extracts and the mixture was kept in the dark for 30 min. Absorbance was measured at 517 nm against a blank whereas, ascorbic acid was used as a positive control.

Statistical analysis

The data was subjected to analysis of variance (ANOVA) using COSTAT computer package (Cohort software, Berkeley, CA, USA). The mean values were compared with the least significance difference (at <0.05) test. One-way ANOVA were performed followed by Duncan S' Multiple Range Test. The values are mean $\pm$ SD and *p*-values (<0.05) were considered as significant.

In silico studies
Dataset collection and molecular docking

The 3 active compounds (cabralealactone, solasodine, and salvadorin) were retrieved from ChemSpider (IDs: 23281688, 391288, and 28282881 respectively) and then converted to

3D Mol2 format using an Open Babel.[31,32] Since the crystal structures of *Rattus norvegicus* cyclooxygenase-2 (COX2) and TNF-α were not present in the protein data bank (PDB) repository, a homology modeling has to be conducted by employing a SwissModel.[33] The crystal structures of murine COX2 (PDB ID: 4FM5) and TNF-α (PDB ID: 2TNF) were selected to model the rat proteins.[34,35] To generate a dimeric structure of TNF-α, individual modeled chains were later recombined as a single PDB coordinate file.

The predicted models were further evaluated based on Procheck, ERRAT, Z-score, and VERIFY 3D.[36–38] The structural alignment of COX-2 and TNF-α homology models on their templates are presented in Figure 1. Subsequently, the AutoDock Vina standard molecular docking procedure was executed as previously documented and analysis of

the binding site was performed before docking.[39–41] COX2 showed high homology 96% with the template, considering a 100% query cover and an E-value of 0.0, while TNF-α was predicted to have a 95% homology, 87% query cover, and an E-value of 6e−10[9]. Superimposition of the co-crystallized structure with inhibitor led to the identification of binding pocket residues. For each protein, docking grid of 30Å × 30Å × 30Å was made covering the binding site residues. Details of the predocking procedure, including protein and ligand preparation, optimization, and minimization were elaborated elsewhere.[42]

Molecular dynamics simulations

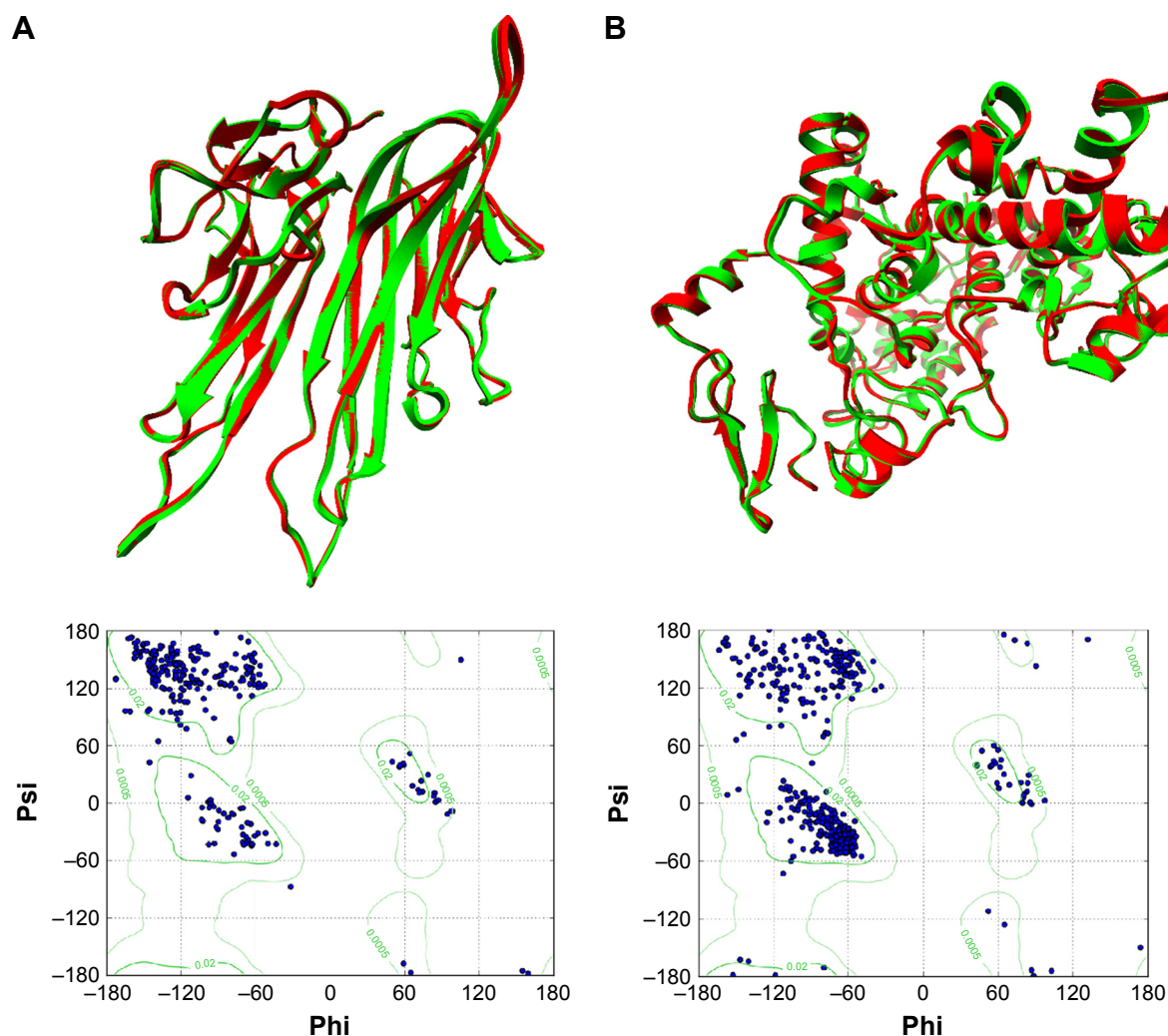The molecular dynamics simulation is performed using an AMBER12 package to gain insight into the conformational

Figure 1 Three-dimensional structural representations of COX-2 and TNF-α, and Ramachandran plot assessment.
Notes: Structural alignment of homology models (in red) of TNF-α (**A**) and COX-2 (**B**) with templates (green) are presented in ribbon representation. Ramachandran plots are shown below for TNF-α and COX-2 in the left and right panels, respectively.
Abbreviations: COX-2, cyclooxygenase-2; TNF-α, tumor necrosis factor alpha.

dynamics of the protein and its binding site during a particular time, and evaluate the validity of the obtained binding mode of ligands from docking calculations.[27,43] In addition, molecular dynamics simulations were used to rid unfavorable forces on the protein to reach equilibrium. The ligand geometry obtained from the docking calculations was used as a starting conformation for molecular dynamics study. Partial charges for ligands were calculated and the force field parameters (force constants for angles and bonds) were used based on the proposed parameters of ANTECHAMBER and General Amber Force Field. Amber ff99SB was also used to provide protein parameters for the modeling.[41] Hydrogen atoms were added by using the t-leap module in Amber16.

The system was solvated to a 10 Å octagonal box of TIP3P water molecules and neutralized by adding an appropriate number of counter ions. The resultant simulation setup was subjected to the MD simulations in the ligand-bound states using the Particle-Mesh Ewald (PME) molecular docking (MD) module in the AMBER 16 MD package. Before the MD simulation of 20 ns, the system was relaxed by performing an energy minimization to remove the largest strains in the system. Then, after heating the system from 0 to 300 K, isotropic position scaling was used to keep the system at a constant pressure (1 atm) while the Berendsen thermostat method was used to maintain a constant temperature (300 K) during the MD simulation. The PME method was used to investigate the contribution of long-range electrostatic interactions. A 10 Å cut-off was used for both PME and van der Waals interactions. To examine the convergence of the system to equilibrium, the temperature, density, and the total energy was checked to ensure post-MD analysis. MD production run of 20 ns was executed for each complex while the Combined Cluster Analysis (CPPTRAJ) module of Amber 16 was used for post-MD analysis.[44]

Results

Significant restoration of the investigated biochemical variables in rat groups that received the herb treatments were seen (Table 2). The biochemical parameters of rats that received monotherapy of salvadorin and solasodin extracts (group H) were significantly ameliorated (41.55±4.34 IU/L, 17.71±1.20 ng/L, 18.01±2.38 pg/mL, 15.20±2.58 ng/mL, 15.41±3.03 pg/mL, 3.65±0.53 nmol/mL, and 1.55±0.386 ng/mL) compared with the control group. In addition, the levels of ALT, AFP, 8-OHdG, TNF-α, IsoP-2a, malondialdehyde (MDA), and COX-2 were significantly improved compared with the control. There remained a significant change in the variables of groups treated with plant extracts. Also, combination therapies of these plant extracts caused significant and remarkable restoration of all parameters compared with the standard drug Clavazin. It is plausible that the antioxidant effect of the plant extracts activate the proteolytic enzymes involved in DNA repair that supports its traditional use as anti-cancer agent.

Histopathological findings

The histopathological findings of the liver sections in the control group (Figure 2A) indicated the presence of visible central veins, a terminal hepatic venule, and an interlobular portal vein. The hepatocytes were in contact with the

Table 2 Biochemical response of cabralealactone, solasodin, salvadorin following CCl₄-induced liver insult in rats

Groups	Mean ± SD (n=10)						
	ALT (IU/L)	AFP (ng/L)	8-OHdG (pg/mL)	TNF-α (ng/mL)	IsoP-2α (pg/mL)	MDA (nmol/mL)	COX-2 (ng/mL)
A	25.11±4.32[f,g]	7.32±3.60[f]	2.88±0.33[e]	20.52±3.95[d]	29.67±2.3[e,f]	1.99±0.60[g]	0.51±0.0016[a]
B	179.82±20.03[a]	92.26±10.60[a]	39.06±10.51[a]	163.55±28.36[a]	171.96±24.44[a]	12.74±1.37[a]	2.09±0.035[b]
C	74.24±11.97[b]	40.87±10.19[b]	29.15±1.90[b]	56.33±6.78[b]	103.56±6.25[b]	6.35±1.52[b,c]	1.60±0.135[d]
D	63.50±5.58[b,c]	37.65±10.82[b]	28.89±5.40[b]	34.30±7.09[c]	87.24±17.81[c]	6.77±1.26[b]	1.75±0.196[d]
E	53.07±7.48[c,d]	43.15±8.80[b]	23.10±3.27[c]	22.79±3.11[c,d]	56.24±6.40[d]	5.41±1.35[b–d]	1.55±0.283[d]
F	42.07±3.25[d,e]	27.31±5.58[c]	18.02±3.30[c]	17.51±1.17[d]	32.47±7.03[e]	4.05±1.30[d–f]	1.67±0.335[d]
G	40.13±2.75[e]	20.494±3.97[c,d]	20.72±2.24[c]	15.41±2.51[d]	19.60±3.72[e–g]	5.09±0.85[c–e]	1.76±0.462[d]
H	41.55±4.34[d,e]	17.71±1.20[d,e]	18.01±2.38[c]	15.20±2.58[d]	15.41±3.03[f,g]	3.65±0.53[e,f]	1.55±0.386[d]
I	20.45±5.05[g]	9.36±1.38[e,f]	8.69±2.08[d]	12.40±1.69[d]	9.84±0.97[g]	2.63±0.59[f,g]	0.62±0.014[a]
J	35.10±8.12[e,f]	10.83±2.56[e,f]	11.92±1.95[d]	12.69±4.00[d]	16.19±2.28[f,g]	3.25±1.22[f,g]	0.82±0.058[c]
LSD (0.05)	11.70	8.87	5.48	12.52	13.89	1.43	1.25
p-value	0.0413	0.011	0.006	0.018	0.007	0.014	0.000

Notes: CCl₄ @ 1 mL/kg b.wt. per week. Cabralealactone, solasodin, salvadorin @ 100 mg/kg b.wt. Clavazin @ 200 mg/kg b.wt. Superscript letters indicate that values not sharing a common letter differ significantly.
Abbreviations: 8-OHdG, 8-hydroxy-2-deoxyguanosine; ALT, alanine aminotransferase; AFP, α-fetoprotein; CCl₄, carbon tetrachloride; COX-2, cyclooxygenase-2; isoP-2α, isoprostanes-2 alpha; LSD, least significance difference; MDA, malondialdehyde; TNF-α, tumor necrosis factor alpha; A, Control; B, CCl₄; C, cabralealactone; D, solasodin; E, salvadorin; F, cabralealactone+solasodin; G, cabralealactone+salvadorin; H, solasodin+salvadorin; I, cabralealactone+solasodin+salvadorin; J, Clavazin.
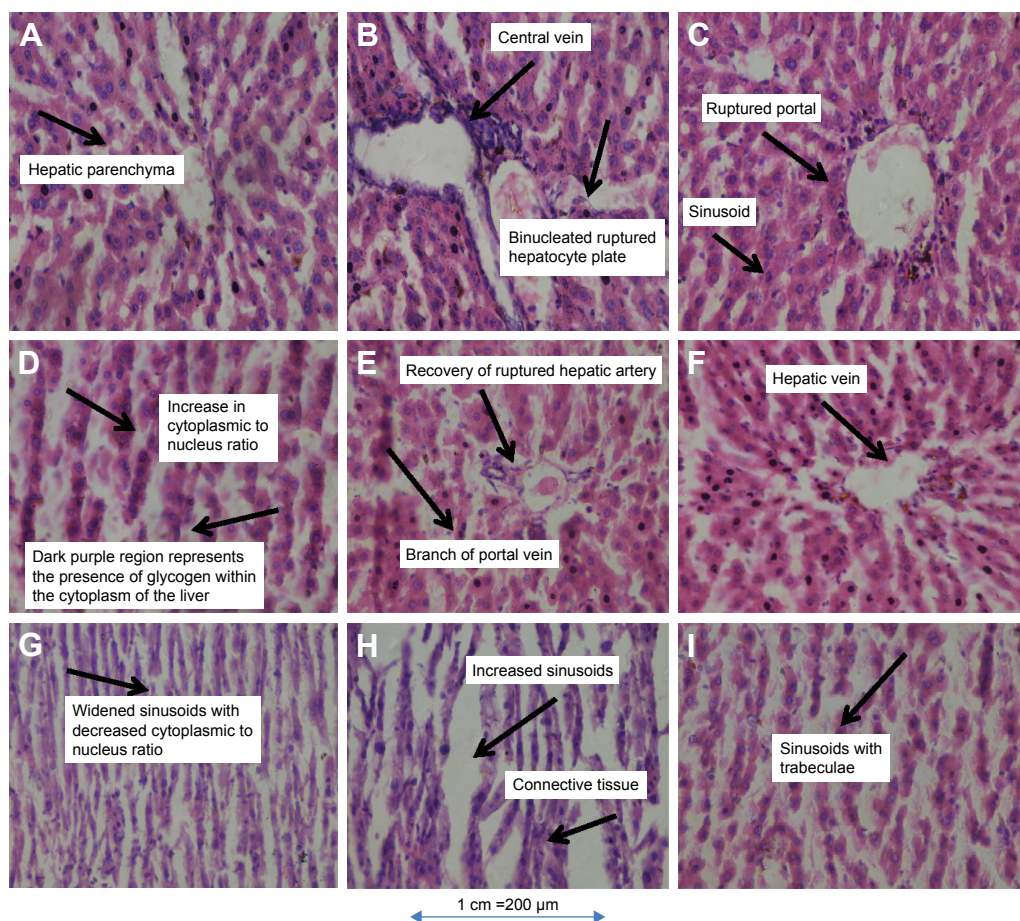
Figure 2 Histopathological findings in rat model. (**A**) Control liver (×40). (**B**) CCl$_4$-treated liver (×40). (**C**) CCl$_4$+cabralealactone-treated liver (×40). (**D**) CCl$_4$+solasodin treated liver (H&E ×40). (**E**) CCl$_4$+salvadorin treated liver (×40). (**F**) CCl$_4$+cabralealactone+solasodin-treated liver (H&E ×40). (**G**) CCl$_4$+solasodin+salvadorin treated liver (×40). (**H**) CCl$_4$+cabralealactone+salvadorin treated liver (×40). (**I**) CCl$_4$+cabralealactone+salvadorin+solasodin treated liver (×40).
Abbreviation: CCl$_4$, carbon tetrachloride.

sinusoids, which appear as distensible vascular channels in connection with highly fenestrated endothelial cells surrounded by a population of phagocytic Kuppfer cells. However, CCl$_4$-treated liver sections indicated the presence of prominent necrosis, vacuolization, central vein congestion, and fat vesicles (Figure 2B). The sinusoids, which are in dilated form, are characteristic of widened hepatic capillaries suggestive of hepatic tumors occurring due to sinusoidal infiltration by malignant or benign cells. The prominent architectural alterations in the CCl$_4$-treated toxic liver are karyomegaly (enlargement of the nucleus) and populated activated Kuppfer cells. Examination of the liver sections in animals treated with standardized extracts of cabralea-lactone (100 mg/kg) revealed that the liver almost regained up to 30% of its normal architecture with reduced intensity of liver fibrosis (Figure 2C). Also, some liver recovery was observed in animals exposed to solasodin (Figure 2D) and salvadorin (Figure 2E) monotherapies as characterized by the lower extent of vacuolization seen.

Nevertheless, compared with the monotherapies, a significantly better protective effect was observed in the liver sections of rats that received combined treatment of standardized extracts of cabralealactone and salvadorin (Figure 2F), cabralealactone and solasodin (Figure 2G), and solasodin and salvadorin (Figure 2H), which were characterized by the presence of normal hepatic cords, absence of fatty infiltration, reduced intensity of sinusoidal dilation, and central vein congestion. However, the best recovery was seen in rat groups exposed to the 3 polyherbal treatment of cabralealactone, salvadorin, and solasodin (Figure 2I), indicating the potentials of these plants as anti-inflammatory agents.

DPPH scavenging activity

Significant DPPH scavenging activity was observed with salvadorin (94.26%) followed by cabralealactone (89.26%) and solasodin (87.06%) compared with ascorbic acid (91.26%) as standards as in Figure 3.
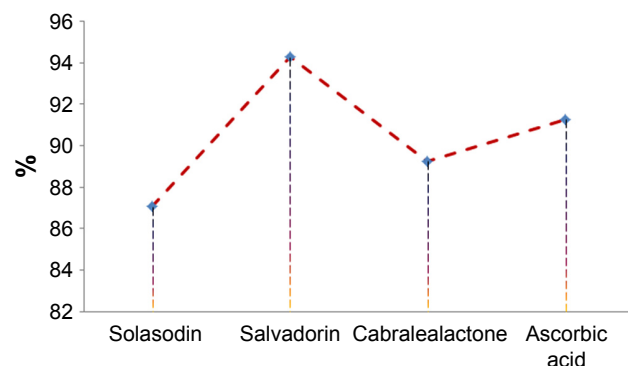
Figure 3 DPPH scavanging activity (%).
Abbreviation: DPPH, 1,1-diphenyl-2-picrylhydrazyl.

In silico studies
Molecular docking and MD simulations

The 3 active compounds were used for molecular docking with COX-2 and TNF-α. The chemical 2D structure representations of the active compounds are shown in Figure 4. The binding energy along with the pharmacokinetics properties of each compound is tabulated in Table 3 while the molecular interactions are diagrammatically represented in Figures 5 and 6. Relative to the COX-2 enzyme, salvadorin exhibited a higher binding energy of −9.8 kcal/mol compared with solasodine and cabralealactone, which showed −7.9 and −6.8 kcal/mol, respectively. In relation

to TNF-α, salvadorin exhibited a potentially higher binding energy of −11.4 kcal/mol, while the binding energies corresponding to solasodine and cabralealactone were −8.1 and −7.4 kcal/mol, respectively. Moreover, all ligands were docked in the lowest energy conformation inside the binding pocket as shown in Figures 5 and 6.

MD simulation of 20 nanosecond (ns) was performed on each lowest docking energy conformation that was chosen as a starting complex for COX-2 and TNF-α. The root mean square deviation (RMSD) of all backbone atoms of each target protein on the bound ligand was computed as a function of time in 1 ns as displayed in Figure 7. Relative to COX-2-salvadorin complex, the RMSD initially increased until 6 ns and then gradually became stable between the mean value of 1.75Å and 2.51Å until the end of the simulation (red), while the RMSD continued to fluctuate between 1.1Å and 2.2Å in the final 10 ns and continued to increase in both cases where COX-2 complexed with solasodine (yellow) and cabralealactone (green). In relation to the TNF-α-salvadorin complex, the backbone atoms RMSD remained stable throughout the 20 ns simulations between 1.15Å and 1.76Å and oscillated around the mean value of 0.51Å. On the other hand, TNF-α-solasodine showed stability in RMSD with small fluctuations while the backbone atoms of TNF-α complexed with cabralealactone showed higher fluctuations and continued to rise
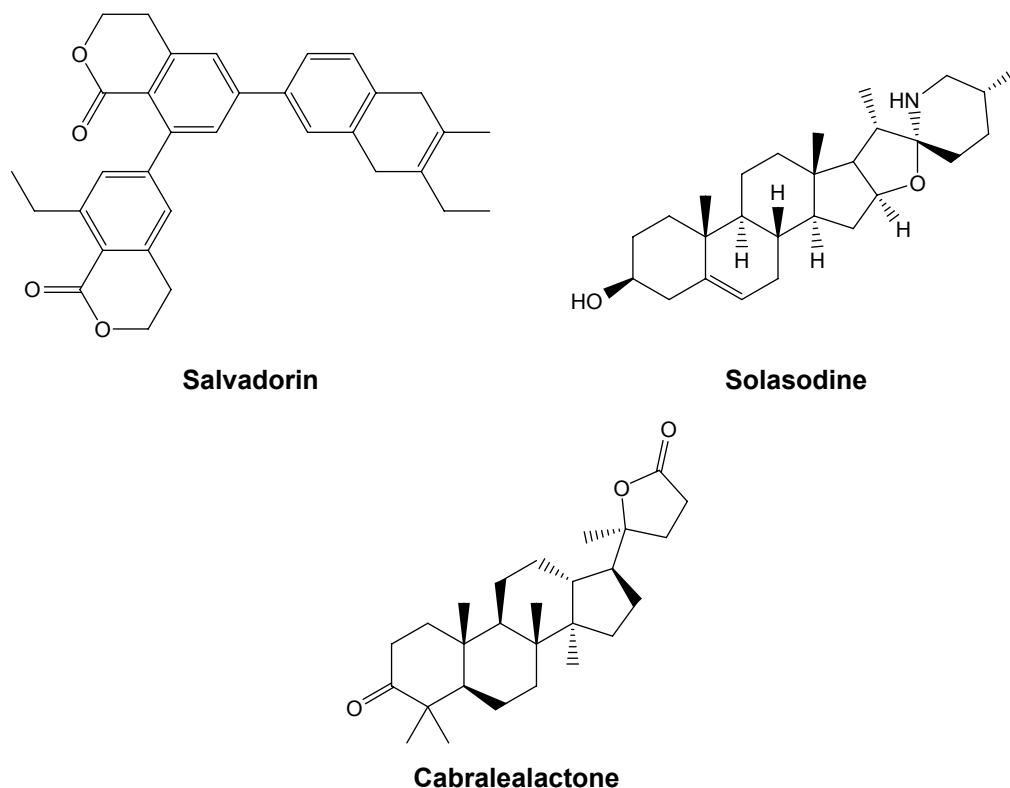

Salvadorin

Solasodine

Cabralealactone

Figure 4 A 2D structure representation of the 3 active compounds.

Table 3 Molecular docking energies and drug-likeness properties of the active compounds

Properties	Cabralealactone	Solasodine	Salvadorin
Mass	552.70	429.68	414.62
Log-p-value	8.69	5.57	6.34
H-bond acceptors	3.00	3.00	3.00
H-bonds donors	0.00	1.00	0.00
Rotatable bonds	5.00	0.00	1.00
PSA	35.53	32.70	43.37
RO5 violations	2.00	1.00	1.00
Atoms	78.00	78.00	72.00
Rings	7.00	6.00	5.00
Binding affinity of compounds (kcal/mol) with COX-2	−6.80	−7.90	−9.80
Binding affinity of compounds (kcal/mol) with TNF-α	−7.40	−8.10	−11.40

Abbreviations: COX-2, cyclooxygenase-2; PSA, polar surface area; RO5, Lipinski's rule of 5; TNF-α, tumor necrosis factor alpha.

until the end; the ligand remained inside the binding pocket of both proteins throughout 20 ns simulation as was evident from the RMSD of salvadorin (black), solasodine (brown), and cabralealactone (orange).

Discussion

To our knowledge, this is the first study to confirm that cabralealactone, solasodin, and salvadorin have DNA-damage protective effects against CCl_4-induced genotoxicity and may have the potential to be investigated as a COX-2 inhibitor and anti-inflammatory agent. The emergence of oxidative stress as a central player in chronic metabolic diseases has opened new avenues for research in the pathology of a wide range of diseases and their treatments to increase the survival rate.[45] The mechanism of action of CCl_4-induced liver damage is a complex mechanism that indicates its absorption in parenchymal hepatocytes and its metabolism results in the formation of free radicals in the presence of cytochrome P_{450}-dependent monooxygenases.[44] The resultant free radicals form a covalent bond with biological macromolecules preferably with fatty acids and phospholipids of the plasma membrane.[46] Once free radicals are produced, lipid peroxidation is initiated, resulting in cellular membrane peroxidation, chloromethylation reaction, polyunsaturated fatty acids (PUFA) deterioration, and ultimately disturbance of the structural integrity. The destruction of phospholipid-associated PUFA leads to physiological alterations in the mitochondria, endoplasmic reticulum, and is mostly prevalent in cellular plasma membrane.[47] In addition to this, the metabolism of calcium-associated homeostasis is disturbed, leading to the loss or leakage of cellular calcium. The resulting end products of PUFA form a covalent association with proteins and mimic the catalytic activity of enzymes.[48,49]
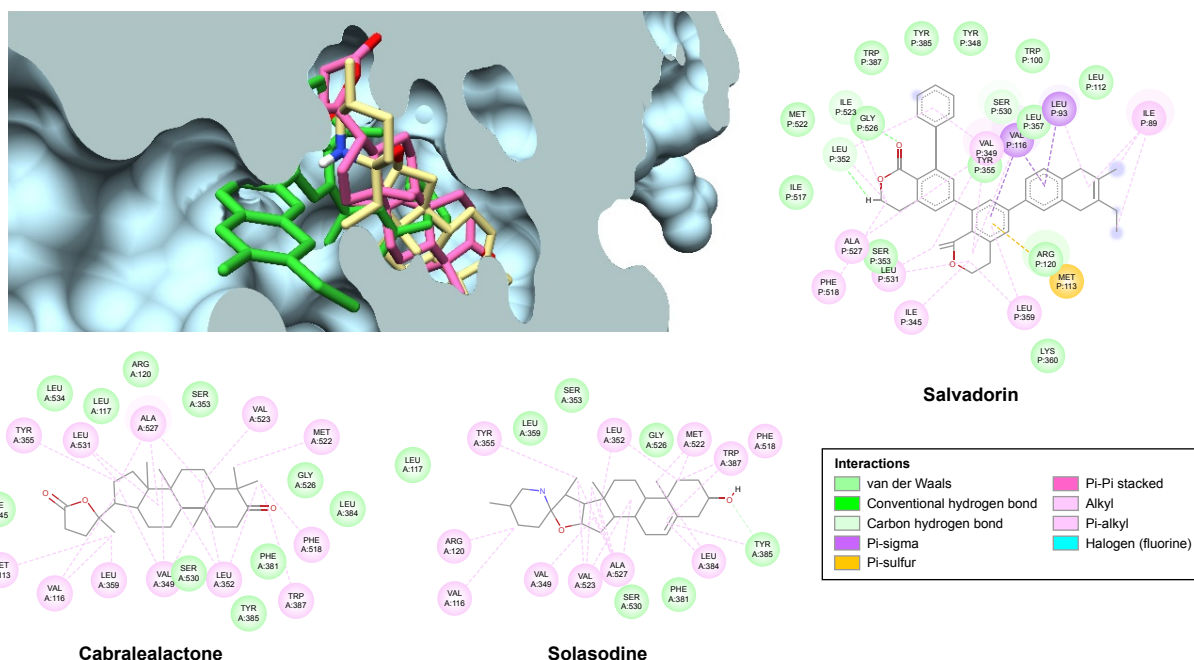

Figure 5 Structure representation of cross-sectional area of COX-2 with docked compounds.
Notes: Cross-sectional area of COX-2 with docked compounds, cabralealactone (pink), solasodine (light brown), and salvadorin (green) in stick representation inside the binding pocket. Molecular interactions in different colors are displayed alongside using a DS visualizer (Accelrys Inc., San Diego, CA, USA).
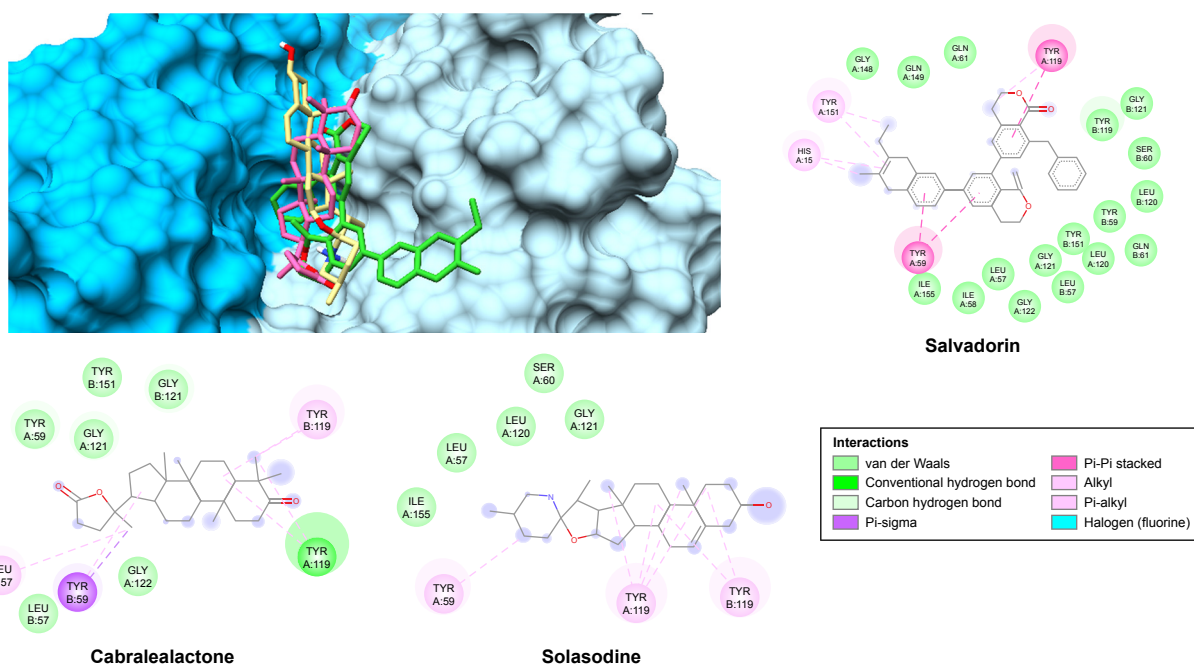**Abbreviation:** COX-2, cyclooxygenase-2.

Figure 6 Molecular surface representation of dimeric TNF-α.
Notes: Molecular surface representation of dimeric TNF-α (in 2 different colors for each chain) with docked compounds, cabralealactone (pink), solasodine (light brown), and salvadorin (green) in stick representation inside the binding pocket. Molecular interactions in different colors are displayed alongside using a DS visualizer (Accelrys Inc., San Diego, CA, USA).
Abbreviation: TNF-α, tumor necrosis factor alpha.

CCl₄ disrupts the cellular integrity by activating inflammatory cytokines such as TNF-α, interleukin (IL)-6, ALT, 8-OHdG (the hallmark of DNA-based oxidative damage, MDA, and isoP-2α). A study reported that patients with raised levels of AFP, histologically increased steatosis, and inflammatory infiltration point to DNA-based oxidative stress.[48] Another research demonstrated that high levels of oxidative stress contribute to dysfunctioning of adipocytokines, leading to dysregulated production of reactive oxygen species from the adipose tissues that caused increased oxidative damage in the blood. This ultimately affected the normal functioning of the liver, skeletal muscles, and aorta of the patients with chronic liver disease.[50,51] The response of cells to the DNA damage is demonstrated via the production of tumor suppressor gene p53 that allows genetic fidelity by inducing cell cycle arrest, ultimately ameliorating the cell damage due to apoptosis as shown in Figure 8.[52,53]

TNF-α is a cytokine with a molecular mass of 55 kDa, which mediates its cytotoxic activities through the expression of 2 receptors (p55 and p75). The induction of reactive oxygen species production by TNF-α occurs via the endothelial mitochondria and nicotinamide adenine dinucleotide phosphate in the cell membrane. Thus, the cytotoxic activity of TNF-α induced by CCl₄ disrupts the hepatocyte mitochondrion function, which stimulates the production of reactive oxygen species in the mitochondria, particularly at the ubiquinone site while TNF-α disrupts the mitochondrial electron transport chain at the complex III region, ultimately resulting in the accumulation of free oxygen radicals inside the mitochondrion. In addition, the increased production of TNF-α also stimulates the nuclear factor-kappa beta activation and upregulated IL-6 expression.

The antioxidant-rich standardized extracts of cabralealactone, salvadorin, and solasodin are useful in repairing the DNA damage and ameliorating the TNF-α-induced cytotoxicity in hepatocytes and malignant transformation of hepatocytes as evidenced by the histological findings. IsoP-2α is recognized as potent indicator of increased oxidative stress in hepatic cirrhosis conditions. The formation of isoprostanes (the isomer of prostaglandin F-2α) is non-enzymatic when free oxygen radicals attack arachidonic acid in the lipid component of the cell membrane. Therefore, isoP-2α is extensively employed as a gold standard index of oxidative stress and DNA damage in liver tissue (Table 4). In our study, high significant correlation exists between some of the aforesaid parameters, which reveals that increased release of ALT from the hepatocytes is responsible for elevated AFP levels in the tissue due to increased production of reactive oxygen species associated with cellular damage, ultimately leading to the DNA damage. Elevated levels of
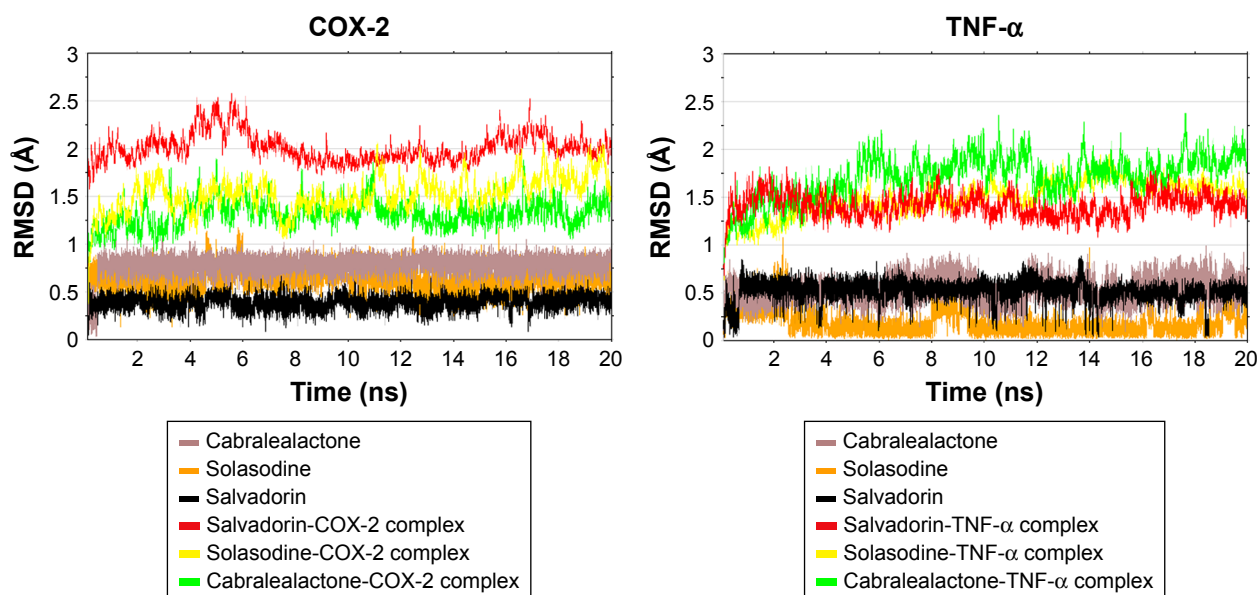
Figure 7 Simulation results of protein-ligand complexes.

Notes: RMSDs during MD simulation of COX-2 and TNF-α of protein-ligand complexes. The RMSDs are plotted as a function of time in 1 ns of the protein backbone of COX-2 and TNF-α with docked ligands during MD simulation at 20 ns. Histopathological findings confirm carbon tetrachloride (CCl_4) induces liver injury by binding to the extracellular receptor which results from the toxic metabolites of CCl_4 causing centrilobular hepatic necrosis and steatosis that disturb the essential cellular processes. CCl_4 is biotransformed by cytochrome P_{450} system in the hepatic microsomes, producing trichloromethyl free radical ($CCl^{-°}_3$) that reacts with cellular molecules and perturb the cellular processes. In the presence of oxygen, $CCl^{°}_3$ is converted to trichloromethyl peroxy radical ($CCl_3OO^{-°}$), resulting in oxidative stress, lipid peroxidation, mitochondrial dysfunction, and loss of membrane integrity. The described model of liver fibrosis indicates that macrophages progress the differentiation and proper functioning of fibroblasts, and act as potent therapeutic agent. Standardized extract of *Cleome brachycarpa* (cabralealactone) suppressed the activation of p53, decreased the expression level of anti-apoptotic protein Bax, and increased the expression level of apoptotic Bcl-2, which resulted in reduced cytochrome C release from the mitochondria into the cytoplasm and inactivated caspases 3 and 9. Ultimately, cabralealactone suppressed fibrosis and necrosis of the hepatocytes. Acute injection of CCl_4 induces hepatocyte necrosis or apoptosis. Damaged hepatocyte release lipid antigens (represented by HSC) resulting in activation of Nk cells. The activated HSC produce a variety of pro-inflammatory cytokines, that is, TNF-α, NF-κβ, IL-6, and COX-2, contributing to hepatocyte inflammation. Treatment of hepatocyte via oral and intraperitoneal injection of standardized extracts of *Solanum incanum* (solasodin) and *Salvadora oleoides* (salvadorin) can attenuate the production of pro-inflammatory cytokines via inhibition of HSC activation and inhibition of the release of cytochrome c oxidase from the mitochondria. Molecular docking studies were carried out to assess the binding affinity of the compounds to proteins, thus mediating tumor growth.

Abbreviations: CCl_4, carbon tetrachloride; COX-2, cyclooxygenase-2; IL, interleukin; MD, molecular docking; HSC, hepatic stellate cell; NF-κB, nuclear factor-kappa beta; RMSD, root mean square deviation; TNF-α, tumor necrosis factor alpha.

AFP may result in the induction of cycle of inflammation; necrosis and regeneration due to CCl_4-induced liver injury. Upregulated cellular turnover in the inflammation cycle and oxidative DNA damage results in the appearance of genetic and epigenetic changes, which may be due to the increased expression of cellular oncogenes and growth and angiogenic factors; activation of telomerase activity; and downregulation of tumor suppressor genes.[54] Nevertheless, the result should be interpreted with caution since AFP has been reported to yield some false-positive findings (20%) in chronic hepatitis C patients and tends to be higher in the presence of liver cirrhosis (20%–50%).[1,55] The current findings corroborated with similar trends seen in the literatures where ALT, MDA, 8-OHdG, AFP, TNF-α, IsoP-2α, and COX-2 levels were elevated. In addition, significant correlation between MDA and 8-OHdG concentrations indicates covalent binding of DNA products with the reactive oxygen species resulting in oxidative DNA damage.

The pyrimidine double bond between C4-C5 is very susceptible to reactive oxygen species, which respond by generating a spectrum of oxidative pyrimidine damage products such as 5-hydroxydeoxyguanosine, thymine glycol, 5-hydroxydeoxycytidine, 8-hydroxydeoxyadenosine, and other purine oxidative products. The production and accumulation of 8-OHdG have been related to carcinogenesis, which causes a decrease in the gene expression and loss of functional integrity of the hepatocytes.[56] Variations in the antioxidant capacity of the standardized extracts of cabralealactone, salvadorin, and solasodin conferred significant amelioration on liver regeneration, survival, and decrease in endogenous DNA damage.

The 3 active compounds were finally subjected to in silico studies to determine the binding potential and stability of protein's all-backbone atoms[57,58] via molecular docking, targeting TNF-α and COX2 enzyme followed by 20 ns MD simulation to analyze the atomistic behavior of protein's backbone with ligand bound inside the binding pocket. Between the 3 compounds, salvadorin yielded the most stable RMSD with minimum fluctuation seen in the final 10–12 ns, which inferred better stability during the formation of the complex (Figure 7). Nevertheless, both in silico and in vivo
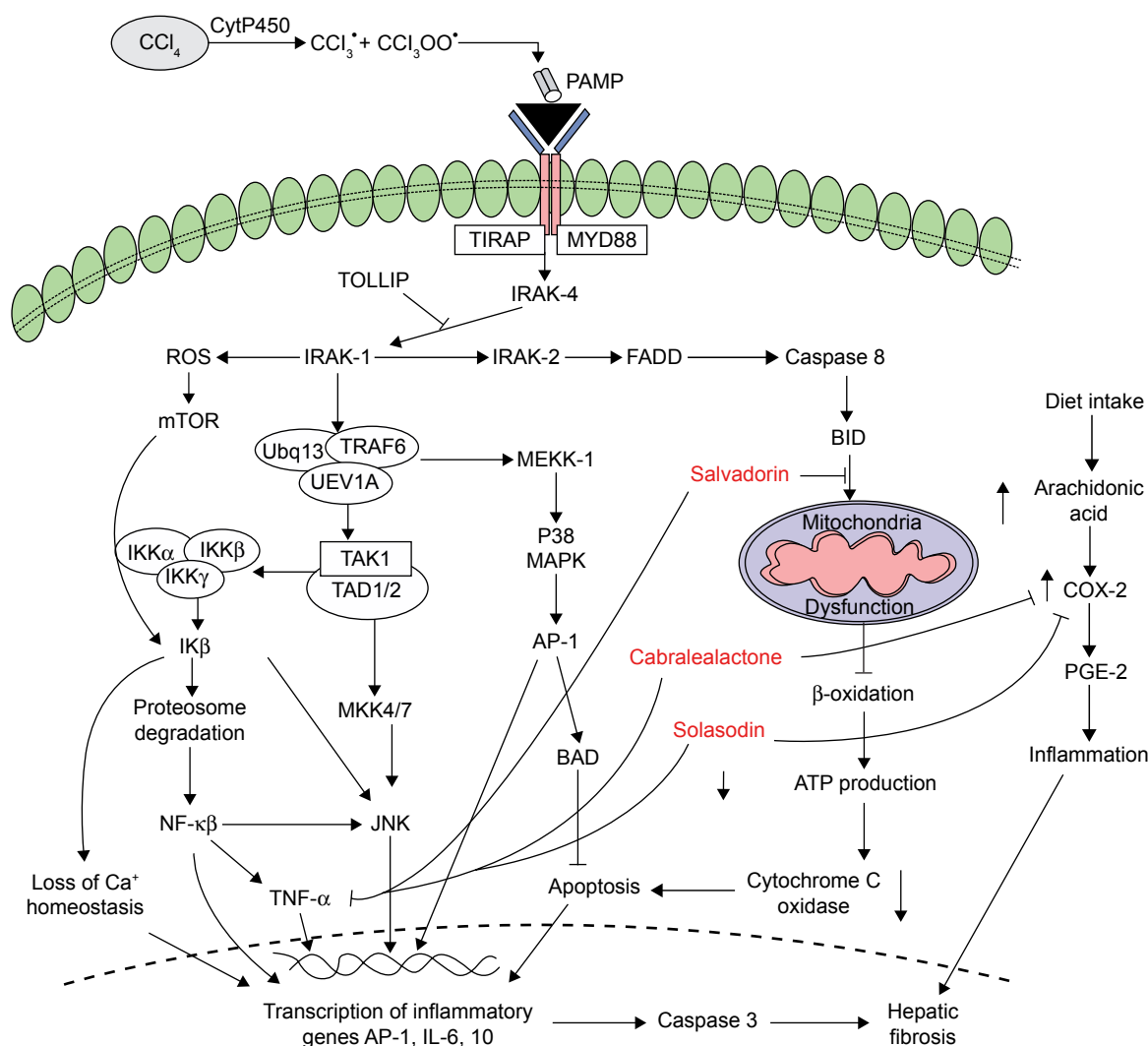
Figure 8 Molecular mechanism involved in the liver damage induced with the carbon tetrachloride (CCl₄).
Abbreviations: CCl₄, carbon tetrachloride; COX-2, cyclooxygenase-2; JNK, Jun N-terminal kinase; MAPK, mitogen-activated protein kinase; NF-κβ, nuclear factor-kappa beta; ROS, reactive oxygen species; TNF-α, tumor necrosis factor alpha.

studies suggested that all 3 active compounds have good and desirable affinity parameters, yielding stable molecular interactions.[59–61] Thus, these compounds can be configured as promising agents for the development of COX-2 and TNF-α antagonists.

Limitations

The limitation of the current study is the relatively low number of samples and variables due to financial constraints. Efficacy of the results can be improved by increasing the number of samples and taken into consideration its molecular level.

Table 4 Pearson correlation coeefficients of different variables in liver tissues of rats under CCL₄ stress receiving cabralealactone, solasodin, salvadorin, and when used in combinations

Variables	ALT	AFP	8-OHdG	TNF-α	IsoP-2α	MDA	COX-2
ALT (IU/L)	1.000	0.913**	0.751**	0.953**	0.905**	0.912**	0.594**
AFP (ng/L)		1.000	0.817**	0.900**	0.889**	0.880**	0.746**
8-OHdG (pg/mL)			1.000	0.714**	0.824**	0.815**	0.699**
TNF-α (ng/mL)				1.000	0.912**	0.884**	0.749**
IsoP-2α (pg/mL)					1.000	0.886**	0.648**
MDA (nmol/mL)						1.000	0.669**
COX-2 (ng/mL)							1.000

Note: **Significant at the 0.01 level (two-tailed).
Abbreviations: 8-OHdG, 8-hydroxy-2-deoxyguanosine; ALT, alanine aminotransferase; AFP, α-fetoprotein; COX-2, cyclooxygenase-2; isoP-2α, isoprostanes-2 alpha; MDA, malondialdehyde; TNF-α, tumor necrosis factor alpha.

Hence, further studies in these areas would be helpful in understanding and raising new sets of ideas in the field.[62–64]

Conclusion

It is concluded that cabralealactone, solasodin, and salvadorin showed hepatoprotective and DNA-damage protective effects against CCl$_4$-induced toxicity. The herbs successfully restored the normal architecture of hepatocytes and had the potential to be used as inhibitor to COX-2 and TNF-α. They can combat oxidative stress and liver injuries when used both as mono and combination therapies, with the later showing better findings perhaps due to synergistic effects.

Acknowledgments

Disclosure

The authors report no conflicts of interest in this work.

References

1. Simonetti RG, Camma C, Fiorello F, Politi F, D'Amico G, Pagliaro L. Hepatocellular carcinoma. A worldwide problem and the major risk factors. *Dig Dis Sci*. 1991;36:962–972.
2. Sies H. Biochemistry of oxidative stress. *Angew Chem Int Engl*. 1986;25:1058–1071.
3. Afifi MS. Phytochemical and biological investigation of *Cleome brachycarpa* Vhel. growing in Egypt. *Int J Pharm Sci Res*. 2014;5(9):4008–4014.
4. Henderson L. Problem plants in ngoro ngoro conservation area. Final Report to the NCAA. 2002.
5. McNeil MJ, Porter RB, Williams LA. Chemical composition and biological activity of the essential oil from Jamaican Cleome serrata. *Nat Prod Commun*. 2012;7(9):1231–1232.
6. Videla LA, Fernandez V. Biochemical aspects of cellular oxidative stress. *Arch Biol Med Exp (Santiago)*. 1988;21:85–92.
7. Gupta NK, Dixit VK. Hepatoprotective activity of *Cleome viscosa* Linn. extract against thioacetamide-induced hepatotoxicity in rats. *Nat Prod Res*. 2009;23(14):1289–1297.
8. Rajaraman R, Saravanan R, Dheeba B, Ramalingam S. In vivo investigation of hepatoprotective activity of *Cleome viscosa* L. in albino rats. *Der Pharmacia Lettre*. 2016;8(3):308–313.
9. Pooryazdani Kojour F, Asgarpanah J, Mahboubi A. In vitro antibacterial activity and total phenolic and flavonoid content of *Cleome brachycarpa* Vahl ex DC methanol extract and its subfractions. *IJGHC*. 2014;3(3):1238–1245.
10. Ali JK, Cheruth AJ, Salem MA, Maqsood S. Evaluation of antioxidant activity of *Cleome brachycarpa* Vahl ex DC, an under-exploited desert plant of United Arab Emirates. *Pharmacology*. 2012;3:167–173.
11. Afifi MS. Phytochemical and biological investigation of *Cleome brachycarpa* Vahl. growing in Egypt. *Int J Pharm Sci Res*. 2015;90:24.
12. Kasai H. Chemistry-based studies on oxidative DNA damage: formation, repair, and mutagenesis. *Free Radic Biol Med*. 2002;33:450–456.
13. Bala A, Kar B, Haldar PK, Mazumder UK, Bera S. Evaluation of anticancer activity of *Cleome gynandra* on Ehrlich's Ascites Carcinoma treated mice. *J Ethnopharmacol*. 2010;129(1):131–134.
14. Son YO, Kim JC, Chung Y. Ripe fruit of *Solanum nigrum* L. inhibits cell growth and induces apoptosis in MCF-7 cells. *Food Chem Toxicol*. 2003;41(10):1421–1428.
15. Fukuhara K, Kubo I. Isolation of steroidal glycoalkaloids from *Solanum incanum* by two counters current chromatographic methods. *Phytochemistry*. 1991;30(2):685–687.
16. Shiu LY, Chang LC, Liang CH. Solamargine induces apoptosis and sensitizes breast cancer cells to cisplatin. *Food Chem Toxicol*. 2007;45(11):2155–2164.
17. Abraham P, Wilfred G, Gathrine SP. Oxidative damage to the lipids and proteins of the lungs, testis and kidney of rats during carbon tetrachloride intoxication. *Clin Chem Acta*. 1999;289:177–179.
18. Sreevidya N, Mehrotra S. Spectrophotometric method for estimation of alkaloids precipitable with Dragendorffs reagent in plant material. *J AOAC Int*. 2003;86(6):1124–1127.
19. Guven A, Gumez M. The effect of kefir on the activities of GSH-Px, GST, CAT, GSH and LPO levels in carbon tetrachloride-induced mice tissues. *J Vet Med B Infect Dis Vet Public Health*. 2003;50:412–416.
20. Bishayee A, Sarkar A, Chatterjee M. Hepatoprotective activity of *Solanum incanum* (thorn apple) against carbon tetrachloride intoxication in mouse liver. *J Ethnopharmacol*. 1995;47(2):69–74.
21. Junnila M, Rahko T, Sukura A, Lindberg LA. Reduction of carbon tetrachloride-induced hepatotoxic effect by oral administration of betaine in male wistar rats: a morphometric histolgic study. *Vet Pathol*. 2000;37(3):231–238.
22. Arora M, Siddiqui AA, Paliwal S, Mishra R. Pharmacognostical and phytochemical investigation of Salvadora oleoides decne. stem. *IJPPS*. 2013;5(Suppl 2):128–130.
23. Saini S, Yadav JP. Antidiabetic and antihyperlipidemic effects of ethanolic extract of *Salvadora persica* L. on Alloxan-induced diabetic rats. *Pelagia Res Lib*. 2013;4(3):178–182.
24. Malik A, Manan A, Mirza MU. Molecular docking and in silico ADMET studies of silibinin and glycyrrhetic acid anti-inflammatory activity. *Trop J Pharm Res*. 2017;16(1):67–74.
25. Ahmed B, Ali AU, Mirza MU. Medicinal plant phytochemicals and their inhibitory activities against pancreatic lipase: molecular docking combined with molecular dynamics simulation approach. *Nat Prod Res*. 2017;1–7.
26. Yousuf Z, Iman K, Iftikhar N, Mirza MU. Structure-based virtual screening and molecular docking for the identification of potential multi-targeted inhibitors against breast cancer. *Breast Cancer (Dove Med Press)*. 2017;9:447–459.
27. Mirza MU, Ikram N. Integrated computational approach for virtual hit identification against ebola viral proteins VP35 and VP40. *Int J Mol Sci*. 2016;17(11):1748.
28. Sharma V, Sarkar IN. Bioinformatics opportunities for identification and study of medicinal plants. *Brief Bioinform*. 2012;14(2):238–250.
29. Kamalakkannan N, Rukkumani R, Aruna K, Varma PS, Viswanathan P, Menon VP. Protective effect of n-acetyl cysteine in carbon tetrachloride-induced hepatotoxicity in rats. *Iran J Pharmacol Ther*. 2005;4:118–123.
30. Reitman S, Frankle S. A colorimetric method for the determination of serum glutamic oxalacetic and glutamic pyruvic transaminass. *Am J Clin Pathol*. 1957;28(1):56–83.
31. Ohkawa H, Ohishi N, Yagi K. Assay for lipid peroxidation in animal tissues by thiobarbituric acid reaction. *Anal Biochem*. 1979;95:351–358.
32. Shimada K, Fujikawa K, Yahara K, Nakamura T. Antioxidative properties of xanthan on the anti-oxidation of soybean oil in cyclodextrin emulsion. *J Agric Food Chem*. 1992;40(1992):945–948.
33. Pence HE, Williams A. ChemSpider: an online chemical information resource. *J Chem Educ*. 2010;87(11):1123–1124.
34. Boyle O, Banck NM, James M, Morley CA, Vandermeersch C, Hutchison TGR. Open babel: an open chemical toolbox. *J Cheminform*. 2011;3(1):33.
35. Schwede T, Kopp J, Guex N, Peitsch MC. SWISS-MODEL: an automated protein homology-modelling server. *Nucleic Acids Res*. 2003;31(13):3381–3385.

36. Windsor MA, Hermanson DJ, Kingsley PJ, et al. Substrate-selective inhibition of cyclooxygenase-2: development and evaluation of achiral profen probes. *ACS Med Chem Lett*. 2012;3(9):759–763.

37. Baeyens KJ, De Bondt HL, Raeymaekers A, Fiers W, De Ranter CJ. The structure of mouse tumour-necrosis factor at 1.4 Å resolution: towards modulation of its selectivity and trimerization. *Acta Crystallogr D Biol Crystallogr*. 1999;55(4):772–778.

38. Laskowski RA, MacArthur MW, Moss DS, Thornton JM. PROCHECK: a program to check the stereochemical quality of protein structures. *J Appl Crystallogr*. 1993;26(2):283–291.

39. Wiederstein M, Sippl MJ. ProSA-web: interactive web service for the recognition of errors in three-dimensional structures of proteins. *Nucleic Acids Res*. 2007;35(2):407–410.

40. Eisenberg D, Lüthy R, Bowie JU. VERIFY3D: assessment of protein models with three-dimensional profiles. *Methods Enzymol*. 1997; 277:396–404.

41. Mirza MU, Mirza AH, Ghori NU, Ferdous S. Glycyrrhetinic acid and E. resveratroloside act as potential plant derived compounds against dopamine receptor D3 for Parkinson's disease: a pharmacoinformatics study. *Drug Des Devel Ther*. 2015;9:187.

42. Mirza MU, Ghori NU, Ikram N, Adil AR, Manzoor S. Pharmacoinformatics approach for investigation of alternative potential hepatitis C virus nonstructural protein 5B inhibitors. *Drug Des Devel Ther*. 2015;9:1825.

43. Trott O, Olson AJ. AutoDock Vina: improving the speed and accuracy of docking with a new scoring function, efficient optimization, and multithreading. *J Comput Chem*. 2010;31(2):455–461.

44. Pearlman DA, Case DA, Caldwell JW, et al. AMBER, a package of computer programs for applying molecular mechanics, normal mode analysis, molecular dynamics and free energy calculations to simulate the structural and energetic properties of molecules. *Comput Phys Commun*. 1995;91(13):1–41.

45. Mirza MU, Rafique S, Ali A, et al. Towards peptide vaccines against Zika virus: ımmunoinformatics combined with molecular dynamics simulations to predict antigenic epitopes of Zika viral proteins. *Sci Rep*. 2016;6:3731–3733.

46. Peters MB, Yang Y, Wang B, et al. Structural survey of zinc-containing proteins and development of the zinc AMBER force field (ZAFF). *J Chem Theory Comput*. 2010;6(9):2935–2947.

47. Roe DR, Cheatham TE III. PTRAJ and CPPTRAJ: software for processing and analysis of molecular dynamics trajectory data. *J Chem Theory Comput*. 2013;9(7):3084–3095.

48. Ozturk F, Ucar M, Ozturk IC, Vardi N, Batcioglu K. Carbon tetrachloride-induced nephrotoxicity and protective effect of betaine in Sprage-Dawley rats. *Urology*. 2003;62(2):353–356.

49. Ohata Y, Ohashi K, Matsura T, Tokunaga K, Kitagawa A, Yamada K. Octacosanol attenuates disrupted hepatic reactive oxygen species metabolism associated with acute liver injury progression in rats intoxicated with carbon tetrachloride. *J Clin Biochem Nutr*. 2008;42(2):118–125.

50. Jeong HG, Park HY. The prevention of carbon tetrachloride-induced hepatotoxicity in mice by α-hederin: inhibition of cytochrome P450 2E1 expression. *Biochem Mol Biol Int*. 1998;45:163–170.

51. Kenan CY, Bulbuloglu E. Improved preservation of erythrocyte antioxidant capacity with ascorbic acid reperfusion after ischemia: a comparative study in rat hind limb model. *Int Journal Altern Med*. 2005;2:1.

52. Ghandrasena LG, Chackrewarthy S, Perera PT, Silva D. Erythrocyte antioxidant enzymes in patients with cataract. *Ann Clin Lab Sci*. 2006; 36:201–204.

53. El-Serag HB, Rudolph KL. Hepatocellular carcinoma: epidemiology and molecular carcinogenesis. *Gastroenterology*. 2007;132:2557–2576.

54. Wang SS, Lu RH, Lee FY, et al. Utility of lentil lectin affinity of alpha-fetoprotein in the diagnosis of hepatocellular carcinoma. *J Hepatol*. 1996;25:166–171.

55. Murugesan GS, Sathishkumar M, Jayabalani R, Binupriya AR, Swaminathani K, Yuri SE. Hepatoprotective and alterative properties of kombucha tea against carbon tetrachloride-induced toxicity. *J Microbiol Biotechnol*. 2009;19(4):397–402.

56. Shieh SY, Ikeda M, Taya Y, Prives C. DNA damage-induced phosphorylation of p53 alleviates inhibition by MDM2. *J Cell*. 1997;91:325–334.

57. Fook-Hong N, Kai-Chiu C, Chi-Sing C. High α-fetoprotein level in HCV-related nodular liver cell dysplasia. *Am J Gastroenterol*. 2011;94: 2296–2297.

58. Hu K, Kyulo N, Lim N. Clinical significance of elevated AFP in patients with chronic hepatitis C, but not hepatocellular carcinoma. *Am J Gastroenterol*. 2004;99:860–865.

59. Rowlinson SW, Kiefer JR, Prusakiewicz JJ, et al. A novel mechanism of cyclooxygenase-2 inhibition involving interactions with Ser-530 and Tyr-385. *J Biol Chem*. 2003;278(46):45763–45769.

60. Orlando BJ, Lucido MJ, Malkowski MG. The structure of ibuprofen bound to cyclooxygenase-2. *J Struct Biol*. 2015;189(1):62–66.

61. Xu L, Stevens J, Hilton MB, et al. COX-2 inhibition potentiates antiangiogenic cancer therapy and prevents metastasis in preclinical models. *Sci Transl Med*. 2014;6(242):242.

62. El-kamali HH, Abdalla BM, Al-Magboul AZ. Antibacterial properties of some essential oils against fine enterobacteriaceae species. *AL-Bututh*. 2007;11(2):11–19.

63. Sarfaraz S, Najam R, Azhar I, Riaz B, Anser H. Anxiolytic and CNS depressant Effects of ethanolic extract of *Cleome brachycarpa* revealed after Neuropharma-cological Screening. *WJPS*. 2014;2(17):605–610.

64. Samejo MQ, Memon S, Bhanger MI, Khan KM. Chemical constituents of essential oil of *Salvadora oleoides*. *J Pharmacy Res*. 2012;5: 2366–2367.